WING-FLAPERON AND SWASHPLATE CONTROL FOR WHIRL-FLUTTER STABILITY AUGMENTATION OF A SOFT-INPLANE TILTROTOR

Rupinder Singh and Farhan Gandhi
The Pennsylvania State University, University Park, PA 16802, USA

Eric Hathaway
The Boeing Company, Philadelphia, PA 19142, USA

Abstract

The effectiveness of active control employed via actuation of the wing-flaperon and the rotor swashplate is examined for improving the whirl-flutter stability characteristics of the soft-inplane Model 222 proprotor on a semi-span wing, over a wide range of variations in airspeed and rotor RPM. Limits are enforced on the magnitude of the control gains utilized based on assumptions on the maximum allowable flaperon/swashplate deflections and the expected magnitudes of the disturbances. Full-state feedback, LQR optimal controllers, scheduled with airspeed and RPM, show large improvements in stability. However, constant-gain and wing-state feedback controllers are attractive due to their simplicity; and the performance of these controllers and their robustness to variations in airspeed and RPM is examined. Results show that for wing-flaperon actuation, constant-gain full-state feedback controllers are robust over a fairly wide RPM range, but the increase in critical flutter speed is smaller than that obtained with scheduled controllers. Wing-flaperon actuation improves the low sub-critical damping in the wing beam mode when based on full-state feedback, but this improvement is not seen when using wing-state feedback. For swashplate actuation, constant-gain full-state feedback controllers are robust over a fairly wide RPM range, and produce an approximately 30-35 knots increase in the critical flutter speed. However, swashplate actuation based on wing-state feedback shows a reduced robustness to variation in RPM suggesting that measurement or estimation of certain rotor states may be required. The robustness of wing-state feedback controllers can be improved if the swashplate actuation limits are increased from ± 1 deg to ± 2 deg. Unlike the flaperon, active control via the swashplate is unable to increase the sub-critical damping in the wing beam mode

Nomenclature

u	=	active control input
δ	=	active flaperon deflection
$[K]$	=	controller gain matrix (or vector)
$\bar{x}$	=	vector of states for the Model-222 proprotor on semi-span wing
w	=	wing tip vertical (beam) bending DOF
v	=	wing tip chordwise bending DOF
ϕ	=	wing tip torsion degree of freedom
b	=	wing vertical (beam) bending mode
c	=	wing chordwise bending mode
t	=	wing torsion mode
$\beta_o, \beta_{1c}, \beta_{1s}$	=	rotor collective, longitudinal cyclic, and lateral cyclic flapping degrees of freedom
$\zeta_o, \zeta_{1c}, \zeta_{1s}$	=	rotor collective, longitudinal cyclic, and lateral cyclic lag degrees of freedom
ψ	=	azimuthal angle
$\dot{\psi}_s$	=	rotor speed degree of freedom
J	=	LQR optimal control cost function
$[Q]$	=	penalty associated with system states in LQR optimal control
R	=	penalty associated with active control inputs in LQR optimal control
$F(K_j)$	=	objective function, moving-point optimization
K_j	=	design variables (control gains)
σ	=	modal damping, % critical
β_G, β, ζ	=	gimbal motion, blade flap and lag motions
θ_a	=	active pitch input through swashplate
F^a	=	aerodynamic load vector due to active control
θ_{1c}, θ_{1s}	=	cyclic pitch inputs to the swashplate
$\lvert\theta_{sp}\rvert$	=	$\sqrt{\theta_{1c}^2 + \theta_{1s}^2}$, magnitude of swashplate tilt
$\dot{(\ )}$	=	time derivative
$(\ )_{sp}$	=	swashplate actuation
$(\ )_{\delta}$	=	flaperon actuation

I. Introduction

Tiltrotor whirl flutter instability has been the focus of considerable analytical and experimental research. The fundamental cause of the instability, destabilizing inplane hub forces generated by the airloads required to precess the rotor, has been well understood for some time. The conventional approach to ensuring adequate whirl flutter stability margins has required wing structures with very

Proceedings of the 31st European Rotorcraft Forum,
Florence, Italy, Sept. 13–15, 2005

high torsional stiffness. This stiffness requirement leads to rather thick wing sections with associated high levels of aerodynamic drag, reducing the aircraft's range and efficiency. While passive design techniques can improve tiltrotor aeroelastic stability, there may be limits to this approach, particularly in the case of softinplane rotor configurations, which are being considered for future tiltrotor designs. For instance, Ref. 1 reported that for soft-inplane tiltrotors, combinations of rotor aeroelastic couplings or wing structural couplings that alleviate air-resonance may be detrimental to whirl flutter stability. Furthermore, the few soft-inplane configurations that have been tested in a wind tunnel (see Refs. 2 and 3) have exhibited unacceptably low levels of wing vertical bending mode damping, which passive design changes alone may not be able to improve. Another option for improving tiltrotor aeroelastic stability is the use of active controls, and there have been several studies that have addressed this subject [2-14].

During a test of the Boeing Model 222 soft-inplane rotor in the NASA Ames 40- by 80-foot wind tunnel, a simple feedback control system to increase damping of the poorly damped wing vertical bending mode was investigated [2]. An accelerometer mounted on the wing tip sensed vertical bending motion of the wing. Active control inputs to the system were introduced through the swashplate. After an open loop study to determine the best gain and phase for the controller, closed loop tests were conducted. The controller was very successful at adding damping to the wing vertical bending mode.

In Ref. 4, Johnson analytically investigated the use of an optimal controller with an estimator for reduction of tiltrotor gust response for both the Boeing and Bell full-scale rotors tested at NASA Ames in the early 1970's. The actuation strategies considered included active flaperons, swashplate inputs, and a combination of the two. Both flaperons and swashplate-based controllers were effective at improving proprotor gust response. Since the lowly-damped wing modes were an important part of the gust response, the controller acted to greatly increase the damping of the wing modes in order to reduce the response. Thus, while Ref. 4 did not explicitly consider the problem of aeroelastic instability, it did confirm that active control was a feasible technique for tiltrotor damping augmentation.

Studies by Nasu [5] and van Aken [6, 7] analytically demonstrated the ability of a simple feedback control system using swashplate actuation to influence whirl flutter stability. No attempt was made in these studies to optimize the performance of the active control system. In Ref. 8, Vorwald and Chopra used optimal control techniques to improve whirl flutter stability. An LQR optimal controller with observer commanding inputs through the swashplate was formulated. A significant increase in predicted flutter speed was obtained, but no consideration was given as to whether the control inputs commanded by the controller were within physically realistic limits.

More recently, a great deal of experimental work [3, 9-11] has been performed at NASA Langley Research Center and Bell Helicopters to evaluate the effectiveness of a modern adaptive control algorithm known as Generalized Predictive Control (GPC) for tiltrotor stability augmentation. GPC is a digital time-domain multi-input, multi-output predictive control method [12]. System identification and control input calculations are performed online. The active control inputs are through the swashplate. These experimental investigations have demonstrated the potential of a GPC-based controller to improve tiltrotor aeroelastic and aeromechanical stability. However, complex adaptive control algorithms such as GPC are not attractive for use in production aircraft due to the high cost of developing and certifying such a system.

From the above, it is evident that tiltrotor active aeroelastic stability augmentation efforts have largely focused on using swashplate-based actuation, with little attention to actuation via a wing-flaperon. An active wing-flaperon, with large control authority in high-speed cruise, is an attractive candidate for increasing tiltrotor whirl flutter stability boundaries, and has been considered for reduction of tiltrotor vibratory loads reduction [15]. Further, while the control algorithms examined varied considerably in terms of sophistication – from simple (even single state) unoptimized feedback controllers, which served to demonstrate the feasibility of active control, to complex adaptive control systems – very limited work has been done with full-state LQR optimal controllers. An LQR optimal controller provides a useful benchmark as it establishes the maximum possible stability augmentation, against which the performance of both simple as well as complex GPC-adaptive controllers can be evaluated. Consequently, the second and third authors of the present article recently, conducted a preliminary study on the effectiveness of a wing-flaperon based actuation system for whirl flutter alleviation, using an LQR optimal control algorithm [13].

Based on the full-scale Model-222 proprotor/semi-span wing model the objectives of the present analytical study are four-fold:

1) To compare the effectiveness of wing-flaperon based actuation versus swashplate-based actuation for whirl flutter stability augmentation of the Model-222 soft-inplane configuration.

2) To examine the robustness of active control, for both actuation concepts, for variations in flight speed and rotor RPM.

3) To examine the effectiveness of simple output feedback controllers, vis-à-vis a full-state optimal controller. How effective is control, based on feedback of a few, key easily-measured wing-states, relative to the performance of a full-state controller?

4) To compare the effectiveness of active control for the soft-inplane configuration to that for a stiff-inplane configuration previously examined by the authors in Ref. 14.

II. Description of Analytical Model and Approach

The analytical model used in the present investigation was developed in Refs. 16 and 17, and its essential features are described briefly. The model represents a single proprotor mounted on a semi-span, cantilevered wing structure. The blades undergo rigid-body flap and lag rotations about spring-restrained offset hinges. The model allows for the distribution of blade flap and lag flexibility inboard and outboard of the pitch bearing. As a result, variations in rotor frequencies and pitch-flap and pitch-lag couplings which occur with changes in collective pitch can be captured from first principles. In contrast, other rigid-blade tiltrotor stability analyses typically rely upon tabulated input data to represent these variations in rotor frequency and couplings. In addition to an in-depth description of the features of the analytical model, and a discussion of the impact of these features on whirl flutter stability prediction, Refs. 16 and 17 provide extensive validation results with existing elastic blade tiltrotor stability analyses as well as experimental test data, for several different tiltrotor configurations. The validated analysis has already been used in initial studies focusing on the influence of a flaperon in alleviating whirl-flutter [13], more detailed studies on whirl-flutter alleviation of the stiff-inplane XV-15 rotor on a semi-span wing [14], as well as detailed design optimization studies to passively improve tiltrotor aeroelastic stability [18]. The wing-flaperon is sized to approximately match the Model-222's flaperon, with a chord equal to 25% of the total wing chord, and a span covering the outer 50% of the wing. A mathematical description of the actuation via an actively controlled wing-flaperon for alleviation of whirl flutter is described Ref. 13. Active control through the swashplate is modeled similarly, and a brief description is provided herewith. The active pitch input via the swashplate is:

$$\theta_a = \theta_{1c}\cos\psi + \theta_{1s}\sin\psi \qquad (1)$$

The aerodynamic loads on the system due to actuation can be written in the form:

for swashplate actuation: $$F_{sp}^a = [D]_{sp}\begin{Bmatrix}\theta_{1c}\\ \theta_{1s}\end{Bmatrix} \qquad (2a)$$

for flaperon actuation: $$F_{\delta}^a = [D]_{\delta}\,\delta \qquad (2b)$$

and using the feedback control law:

for swashplate actuation: $$\begin{Bmatrix}\theta_{1c}\\ \theta_{1s}\end{Bmatrix} = -[K]_{sp}\,\bar{x} \qquad (3a)$$

for flaperon actuation: $$\delta = -[K]_{\delta}\,\bar{x} \qquad (3b)$$

leads to:

for swashplate actuation: $$F_{sp}^a = -[D]_{sp}[K]_{sp}\,\bar{x} \qquad (4a)$$

for flaperon actuation: $$F_{\delta}^a = -[D]_{\delta}[K]_{\delta}\,\bar{x} \qquad (4b)$$

Equations 4a and 4b can be represented, together, as:

$$F^a = -[D][K]\bar{x} \qquad (5)$$

The matrix $[D]$ contains contributions from aerodynamic terms, $[K]$ represents the controller gain matrix and $\bar{x}$ is the vector of rotor/wing states. While the flaperon deflection, δ, is a scalar, the total deflection (or "tilt") of the swashplate due to the active cyclic pitch inputs is given as:

$$|\,\theta_{sp}\,| = \sqrt{\theta_{1c}^a + \theta_{1s}^a} \qquad (6)$$

A. Limits on Control Gains

An important issue in evaluating the effectiveness of an active control scheme is actuation authority. A given set of controller gains may be able to completely eliminate whirl flutter, but if the controller commands flap deflections or swashplate inputs that exceed the practical limits, then the performance improvements predicted (increase in whirl flutter critical speed or increase in damping of specific modes) have no practical significance. Limits on the controller gains can be introduced by considering both the magnitude of perturbations the system is likely to encounter as well as the limits on the flaperon and swashplate deflections, themselves. Based on Ref. 15, it is assumed that nominally the available flaperon deflection for stability augmentation is ± 6 deg, and the available swashplate motion is ± 1 deg.

The impact of higher limits for the wing-flaperon/swashplate input on the controller performance is also examined in the present study. These higher limits correspond to ± 10 deg flaperon deflection and ± 2 deg swashplate motion.

The feedback control laws for swashplate and flaperon actuation were given in Eqs. 3a and 3b, and can be expressed generally as:

$$u = -[K]\bar{x} \qquad (7)$$

where u represents the swashplate inputs, $\lfloor \theta_{1c} \quad \theta_{1s} \rfloor^T$, or the flaperon deflection, δ. It is evident that for a specified maximum limit on u the controller gain matrix $[K]$ is limited by $\bar{x}$. The larger the disturbance levels (larger $\bar{x}$), the tighter the limits on the controller gain matrix, and vice-

versa. Thus, for a controller designed for practical implementation, a worst-case disturbance condition must be identified, and controller gains limited to prevent the control input, u, from exceeding the prescribed limits for this disturbance. The state vector, $\bar{x}$, corresponding to the Model-222 semi-span model is given by

$$\bar{x} = \begin{bmatrix} \dot{w} & \dot{v} & \dot{\phi} & \dot{\beta}_o & \dot{\beta}_{1c} & \dot{\beta}_{1s} & \dot{\zeta}_o & \dot{\zeta}_{1c} & \dot{\zeta}_{1s} & \dot{\psi}_s \\ w & v & \phi & \beta_o & \beta_{1c} & \beta_{1s} & \zeta_o & \zeta_{1c} & \zeta_{1s} \end{bmatrix}^T \quad (8)$$

For the present study it is assumed that disturbances would cause the following maximum wing tip deformations for the semi-span tiltrotor model: Wing tip displacements of 2.5% of the rotor radius vertically, 1% of rotor radius in the chordwise direction, and torsional rotation of 1 degree. The control gains selected for the results in this study ensure that for the perturbations considered above, the resulting wing-flaperon/swashplate inputs do not exceed the maximum limits placed on them.

B. Evaluation of Optimal Controller Gains

An LQR optimal controller is implemented which determines a set of controller gains that minimizes the following cost function:

$$J = \int_0^\infty (\bar{x}^T [Q] \bar{x} + u^T R u) dt \quad (9)$$

where $\bar{x}$ is the state response vector, and u represents flaperon/swashplate actuation inputs. The value of the weight on control effort, *R,* is iteratively adjusted to allow the largest possible increase in flutter speed, without exceeding the actuation limits described previously. The optimal controller gains depend on the plant or model parameters, which vary, for example, with flight speed or RPM. Thus, the best performance is obtained for a controller that is scheduled with respect to airspeed and RPM. However, this increases the complexity of the controller, and it would be very advantageous if a constant gain controller were effective over a broad range of conditions (implying that the controller is robust to variations in operating condition).

C. Moving-Point Optimization Scheme

To alleviate the possibility that a controller that is optimal at one condition performs poorly off-design, a moving-point optimization procedure is used to determine a control gain matrix that stabilizes the least damped mode over a range of variation in RPM. The algorithm that is used is similar to that developed in Refs. 18-20 (also used by the authors in Refs. 14 and 18), and is described briefly herewith.

Formal optimization procedures were used with the goal of determining a combination of the design variables that will alleviate whirl flutter throughout the RPM range under consideration (300-600 RPM). This range extends from about 85 RPM below the cruise value through about 50 RPM greater than the hover value of the Model-222 rotor, to provide a broader insight into the controller performance. The design variables considered were the constant (non-scheduled) control gains. The optimization procedure attempts to increase the level of damping in the *least* damped mode by minimizing the following objective function:

$$\text{minimize} \quad F(K_j) = -\sigma_{min}\Big|_{RPM = 300 \rightarrow 600} \quad (10)$$

where K_j are the control gains (design variables) and σ_{min} is the damping corresponding to the least damped mode at any iteration in the optimization process. As the values assigned to the various design variables change during the optimization process, the identity of the least damped mode, as well as the RPM at which it occurs, varies. Therefore, for each iteration in the optimization procedure, the RPM corresponding to σ_{min} is determined and the optimization process is continued at this RPM. The sensitivity gradients, $\partial\sigma_{min} / \partial(K_j)$, are calculated numerically by individually perturbing each of the design variables. This process is repeated until optimality is achieved. This procedure yields a controller design that is sub-optimal at any *single* RPM, but ensures a degree of robustness for variation in RPM. The process described here can, in principle, be extended to determine control gains that are robust to variations in other operational parameters such as airspeed and plant parameters such as rotor/wing frequencies. It should also be noted that the design variables, K_j (the controller gains being evaluated), are a subset of $[K]_{sp}$ and $[K]_\delta$ in Eqs. 3 and 4 when output feedback (based on a few states) is used.

III. Results

A. Baseline Results – No Control

Numerical simulations are presented for the soft-inplane Model-222 rotor on a semi-span wing model, the essential features of which have been described in Ref. 2. Properties of this configuration are also conveniently found in Ref. 16.

Figures 1 and 2 show the plots of the baseline modal damping (no active control), as a function of airspeed, at the rotational speeds of 386 RPM (the cruise RPM of the Model-222 proprotor) and 551 RPM (the hover RPM of the Model-222 proprotor), respectively. At the cruise RPM (Fig. 1) whirl flutter instability is encountered at a speed of 390

knots, and at the hover RPM (Fig. 2) instability is encountered at 395 knots. The wing chordwise bending mode is the critical mode at the cruise RPM and the wing torsion mode is the critical mode at the hover RPM. The low level of sub-critical damping of the wing vertical bending mode at the cruise RPM may be observed on Fig. 1. Figure 3 shows the modal damping variation, as a function of RPM, at an airspeed of 410 knots (an arbitrarily selected target cruise speed at which it is desired that the system, with the introduction of active control, be free of whirl-flutter instability). Since this speed is greater than the critical flutter speeds for the baseline (no control) system at either the cruise or the hover RPM, certain modes are seen to have negative damping.

B. Full-State LQR Control – Airspeed-scheduled and Constant Gain Controllers

Wing-Flaperon Actuation

Influence of wing-flaperon actuation based on full-state LQR optimal control is shown in Figs. 4 and 5, for the 386 RPM and 551 RPM cases, respectively. In both figures the optimal control gains are scheduled with respect to airspeed. Full-state LQR optimal control ensures stability, so the damping in the various modes never becomes negative. The critical flutter speed, then, is the speed at which the flaperon deflections required exceed the prescribed limits (nominally assumed to be ± 6 deg). The value of the weighting parameter R is adjusted iteratively, to simultaneously increase the critical flutter speed and maintain greater than about 1% damping in the three wing modes. At the cruise RPM (Fig.4) the stability boundary is increased to 435 knots, at which point the flaperon deflections exceed the ± 6 deg limit. This represents a 45 knot increase over the 390 knot critical flutter speed for the baseline system at cruise RPM (Fig. 1). A higher ± 10 deg flaperon deflection limit would increase the critical flutter speed to about 445 knots – a 55 knot increase over the baseline. There is also an increase in the sub-critical wing vertical bending mode damping (compare Fig. 4 to Fig. 1). At the hover RPM (Fig. 5) the flaperon deflections do not exceed the ± 6 deg limit up to the 500 knots upper limit on airspeed considered.

Next, from Fig. 4 (corresponding to the cruise RPM) the optimal gains at 410 knots airspeed are applied over the entire airspeed range, at cruise (386) and hover (551) RPM. The corresponding modal damping values, as a function of airspeed, are shown in Figs. 6 and 7. At 386 RPM (Fig. 6) it is seen that flutter is encountered at around 420 knots, at which point the regressive flap, wing chord, and wing beam modes approach zero damping. This represents an increase of 30 knots over the baseline value of 390 knots (compare to Fig. 1), and the flaperon deflections are less than ± 6 deg at sub-critical speeds. The increase in the level of sub-critical wing vertical bending mode damping, seen in Fig. 4, is also preserved. The corresponding increase in flutter speed when the same control gain vector is applied at the hover (551) RPM (see Fig. 7) is about 15 knots (up from a baseline value of 395 knots in Fig. 2 to 410 knots, at which point the flaperon deflections exceed the ± 6 deg limit).

Figure 8 shows the effect of the cruise-RPM 410-knot optimal gain vector (used in Fig. 6 and Fig. 7) over the 300-600 RPM range considered (at 410 knots airspeed). All modes are observed to be stable over a large portion of the RPM range (from 375 RPM onwards, which includes both the cruise and hover RPM values). Clearly, a constant gain controller performs reasonably well over a large portion of the RPM range, (compare the results in Fig. 8 to the baseline in Fig. 3), and over the airspeed range at either cruise or hover RPM (compare results in Fig. 6 and Fig. 7 to those in Fig. 1 and Fig. 2 respectively). The flaperon deflections corresponding to Fig. 8 remain below the ± 6 deg limit throughout the 300-600 RPM range.

Swashplate Actuation

For the case of swashplate actuation, performance of the optimal LQR controller scheduled with airspeed is shown in Figs. 9 and 11. At the cruise RPM (Fig. 9) the stability boundary is increased by about 30 knots, from the baseline value of 390 knots (Fig. 1) to about 420 knots, at which point the ± 1 deg limit on swashplate input is exceeded. Corresponding to cruise RPM (Fig. 9) Fig. 10 shows the swashplate deflections when the wing beam, chord and torsion modes are excited (to their maximum values previously specified). While the ± 1 deg limit on the swashplate deflection is exceeded at 420 knots (when the torsion mode is excited to its maximum amplitude), a higher maximum swashplate deflection of ± 2 deg is exceeded only at 475 knots (again due to wing torsion mode perturbations). Unlike the flaperon actuation case (Fig. 4) no appreciable increase in sub-critical damping of wing vertical bending mode is observed, relative to the baseline system (Fig. 1). At the hover RPM (Fig. 11), the increase in critical flutter speed is about 55 knots, from the baseline value of 395 knots (Fig. 2) to about 450 knots, at which point again the swashplate actuation limit of ± 1 deg is exceeded. The corresponding swashplate deflections (when the wing beam, chord, or torsion modes are excited to their maximum levels) are shown in Fig. 12. The ± 2 deg limit is not exceeded at any value of airspeed, for the hover RPM case.

Next, from Fig. 9 (corresponding to the cruise RPM) the optimal gains at 410 knots airspeed are applied over the entire airspeed range, at the cruise RPM. The corresponding modal damping values, as a function of airspeed, are shown in Fig. 13. It is seen that flutter is encountered at around 425 knots, at which point the regressing flap, progressing flap and wing chord modes approach zero damping. This represents an increase of 35 knots over the baseline value of 390 knots (compare to Fig. 1). The sub-critical wing vertical bending mode damping is, again, poor. When these gains are applied at the hover RPM (Fig. 14) a 30 knot increase in flutter speed is observed (up to 425 knots, compared to the

baseline value of 395 knots in Fig. 2). At this point the wing torsion mode becomes unstable. For both Fig. 13 and Fig. 14, the swashplate deflections remain below the ± 1 deg limit at all airspeeds in the sub-critical range. The results of Figs. 13 and 14 show that a constant gain controller (using gains which were optimal at 410 knots and 386 RPM) performs comparably to airspeed or RPM scheduled controllers.

Figure 15 shows the effect of the cruise-RPM 410-knot airspeed optimal gains (used in Fig. 13 and Fig. 14) over the 300-600 RPM range considered (at 410 knots airspeed). All modes are seen to be stable from 370-575 RPM, which includes both the cruise and hover RPM of the Model-222 proprotor. Thus, a constant set of controller gains is able to increase flutter speed at both cruise and hover RPM values, and shows good robustness to variation in RPM.

Overall, the above observations are similar to those for the stiff-inplane XV-15 rotor on a semi-span wing (Ref. 14), but the increase in critical flutter speed is smaller (nearly 25 kts as oppsed to 70-90 kts for the XV-15). This, however, may be because the baseline flutter speed for the Model 222 is higher (390-395 kts, compared to 315–330 kts for the XV-15).

C. Moving-Point Optimization with Wing-State (Output) Feedback

In this section controllers based on feedback of a few key states are examined. This is because output feedback of a few easily-measured states is more practical than full-state feedback. Further, in the LQR optimal control gain vectors (for flaperon-based control) and the LQR optimal control gain matrices (for swashplate-based control), it was observed that the gains corresponding to the six wing states (wing tip positions, w, v and ϕ, and velocities $\dot{w}$, $\dot{v}$ and $\dot{\phi}$) were the dominant gains. This raised the possibility that the performance of a controller based on the feedback of wing states alone may be competitive to that of a full-state feedback controller. The constant controller gains are evaluated using a moving-point optimization scheme over the 300 – 600 RPM range, at an airspeed of 410 kts.

Wing-Flaperon Actuation

For the wing-flaperon actuation case, Fig. 16 shows the results of a wing-state feedback controller designed using a moving-point optimization over a range of 300-600 RPM (and 410 knot airspeed). All modes are seen to be stable for rotor speeds greater than 375 RPM (below which the regressing flap mode first goes unstable). For the results shown in Fig. 16, the flaperon deflections remain less than the ± 6 deg limit. In terms of RPM range over which the system remains stable, the performance of an output feedback control scheme based on wing states alone is comparable to the performance of a full-state feedback controller (compare Fig. 16 to Fig. 8). Similar observations for the stiff-inplane XV-15 case, on comparable robustness of wing-state and full-state feedback controllers to variations in RPM, when using flaperon actuation, are reported in Ref. 14. However, the increase in sub-critical damping of the wing beam mode at cruise RPM, seen with full-state feedback, was not observed with wing-state feedback alone.

Figures 17 and 18 show modal damping versus airspeed at the cruise RPM and hover RPM respectively, using the controller gains of Fig. 16. At the cruise RPM (Fig. 17), the critical whirl flutter speed is 405 knots – which represents a more modest 15 knot increase over the baseline (Fig. 1). The flaperon deflections remain within their prescribed limit of ± 6 deg for this case. Despite the slight increase in critical flutter speed the sub-critical wing vertical bending mode damping is very low (compare Fig. 17 to Fig. 1). At the hover RPM (Fig. 18), the critical whirl flutter speed is 480 knots – which represents a significant 85 knot increase over the baseline (Fig. 2), with the critical flutter speed being determined by the airspeed at which the flaperon deflections exceed the ± 6 deg limit.

Scaling up the control gains of Fig. 17 for allowable flaperon deflections of ± 10 deg did not show appreciable improvement in modal damping (results not presented).

Swashplate Actuation

For the case of swashplate actuation, Fig. 19 shows the results of a wing-state feedback controller designed using a moving-point optimization over a range of 300-600 RPM (and 410 knot airspeed). The controller gains thus determined result in the modes being stable over a range of 400-515 RPM (a limited range that includes neither the cruise nor the hover RPM of the Model-222). The wing torsion mode becomes unstable at rotational speeds higher than 515 RPM. Comparing the results in Fig. 19 to those in Fig. 15 (corresponding to full-state feedback with gains which are optimal at 410 knots, at 386 RPM), it is evident that with swashplate actuation, an output feedback controller (based on measurement of wing states alone) does not have the robustness of a full-state controller. This is in contrast to the flaperon actuation case, where output feedback (based on measurement of wing states) resulted in no major degradation in robustness (as seen from a comparison of Figs. 8 and 16). In Ref. 14, a similar observation was made for the stiff-inplane XV-15 case – that to have the best performance with the swashplate as the actuation mechanism, measurement or estimation of some rotor states may be required.

If the control gains of Fig. 19 are scaled up for allowable swashplate deflections of ± 2 deg, this results in stability of all modes from 370-600 RPM (at 410 knots airspeed), as shown in Fig. 20. This suggests that although wing-state feedback control may not be robust to variations in RPM when the swashplate actuation limit is small (± 1 deg), the robustness is improved if larger actuation inputs (± 2 deg) are possible. This is again similar to the observation made for the XV-15 case in Ref. 14.

IV. Conclusions

For the baseline configuration (no control), the critical flutter speed was determined to be 390 kts at the cruise RPM (386 RPM), and 395 kts at the hover RPM (551 RPM). Further, at the cruise RPM, the wing beam mode damping was very low even at sub-critical speeds. Since the critical flutter speed is fairly high (compare to the stiff-inplane XV-15 configuration, Ref. 14, where it was 315 – 330 kts), success of the active controller could be evaluated as much by its ability to increase the sub-critical wing beam mode damping as by its ability to increase the critical flutter speed.

Full-State Feedback – Flaperon Actuation: Using scheduled LQR optimal controllers at the cruise and hover RPM values results in large increases in flutter speed (from 390 to 435 kts at the cruise RPM, and from 395 all the way up to the 500 kt maximum speed considered at the hover RPM). The 435 kt critical speed at cruise RPM is determined by flaperon deflections exceeding the ± 6 deg limit, and would go to 455 kts if the allowable flaperon deflection increased to ± 10 deg. The controller was able to substantially increase the sub-critical damping in the wing beam mode. When controller gains optimal at the cruise RPM and a 410 kt airspeed are applied throughout, this constant gain controller shows reasonably good robustness over a wide range of RPM variation at 410 kts airspeed, but increases in critical flutter speed are much more modest – up 420 kts at the cruise RPM and to 410 kts at the hover RPM. This is in contrast to the observation for the XV-15 stiff-inplane configuration in Ref. 14, where constant gain controllers were found to be comparable in performance to the scheduled LQR optimal controllers. For the Model 222, the increase in sub-critical wing beam mode damping at cruise RPM is preserved with the constant gain controller.

Full-State Feedback – Swashplate Actuation: Using scheduled LQR optimal controllers at the cruise and hover RPM values results in increases in flutter speed from 390 to 420 kts at the cruise RPM, and from 395 to 450 kts at the hover RPM. The critical speeds are determined by swashplate deflections exceeding the ± 1 deg limit, and would go to 475 kts at the cruise RPM, and to beyond 500 kts at the hover RPM, if the allowable swashplate deflection increased to ± 2 deg. *Unlike the flaperon, active control via the swashplate was unable to increase the sub-critical damping in the wing beam mode*. When controller gains optimal at the cruise RPM and a 410 kt airspeed are applied throughout, the critical flutter speed is found to be 425 kts at both the cruise and hover RPM. The critical speed is defined by modes going unstable (as opposed to swashplate deflections exceeding the prescribed limit). At a 410 kt airspeed, all modes are seen to be stable from 370-575 RPM, which includes both the cruise and hover RPM of the Model-222 proprotor. Overall, constant gain controllers show good robustness and comparable performance improvements (increases in flutter speed) to scheduled LQR optimal controllers. Similar observations were made for the XV-15 proprotor/wing configuration in Ref. 14.

Wing-State Feedback – Flaperon Actuation: A moving-point optimization was carried out at 410 kts airspeed to determine control gains that stabilize the system over a 300–600 RPM range. Stability was observed over the 375–600 RPM range, which includes both the cruise and hover RPM values, while respecting the ± 6 deg flaperon deflection limit. The increase in critical flutter speed at cruise RPM is a modest 15 kts, up to 405 kts, but is more impressive at the hover RPM – up to 480 kts. It should be noted that at the cruise RPM, active control using wing-state feedback is unable to improve the sub-critical wing beam mode damping (in contrast to full-state feedback).

Wing-State Feedback – Swashplate Actuation: Using a moving point optimization over a 300–600 RPM range (and 410 kt airspeed) returned control gains that resulted in modes being stable only over a 400–515 RPM range (a limited range that includes neither the cruise nor the hover RPM of the Model-222). This reduction in robustness to variation in RPM (compared to full-state feedback) suggests that if the swashplate is used for active control, measurement or estimation of some rotor states may be required. However, if the permissible swashplate inputs are increased to ± 2 deg, robustness to variation in RPM improves considerably. The above observations are consistent with those made for the XV-15 in Ref. 14.

Acknowledgments

This research is funded by the National Rotorcraft Technology Center (NRTC) under the Penn State Rotorcraft Center of Excellence Program, with Dr. Yung Yu serving as the technical monitor.

References

1. Howard, A. K. T., *The Aeromechanical Stability of Soft-Inplane Tiltrotor*s, Ph.D. thesis, The Pennsylvania State University, 2001.
2. Magee, J. P. and Alexander, H. R., "Wind Tunnel Tests of a Full Scale Hingeless Prop/Rotor Designed for the Boeing Model 222 Tilt Rotor Aircraft," NASA CR 114664, Boeing Vertol Co., Oct.1973.
3. Nixon, M. W., Langston, C. W., Singleton, J. D., Piatak, D. J., Kvaternik, R. G., Corso, L. M., and Brown, R. K., "Aeroelastic Stability of a Four-Bladed Semi-Articulated Soft-Inplane Tiltrotor Model," Proceedings of the 59th Annual AHS Forum, Phoenix, Arizona, May 6–8, 2003.

4. Johnson, W., "Optimal Control Alleviation of Tilting Proprotor Gust Response," *Journal of Aircraf*t, vol. 14, no. 3, March 1977, pp. 301–308.
5. Nasu, K.-i., "Tilt-Rotor Flutter Control in Cruise Flight," NASA TM 88315, December, 1986.
6. van Aken, J. M., "Alleviation of Whirl-Flutter on Tilt-Rotor Aircraft Using Active Controls," Proceedings of the 47th Annual AHS Forum, Phoenix, AZ, May 6–8, 1991.
7. van Aken, J. M., "Alleviation of Whirl-Flutter on a Joined-Wing Tilt-Rotor Aircraft Configuration Using Active Controls," Presented at the International Specialists' Meeting on Rotorcraft Basic Research of the American Helicopter Society, Atlanta, Georgia, March 25–27, 1991.
8. Vorwald, J. G. and Chopra, I., "Stabilizing Pylon Whirl Flutter on a Tilt-Rotor Aircraft," Proceedings of the 32nd AIAA/ASME/ASCE/AHS/ASC Structures, Structural Dynamics, and Materials Conference, Baltimore, MD, April 8–10, 1991.
9. Kvaternik, R. G., Piatak, D. J., Nixon, M. W., Langston, C. W., Singleton, J. D., Bennett, R. L., and Brown, R. K., "An Experimental Evaluation of Generalized Predictive Control for Tiltrotor Aeroelastic Stability Augmentation in Airplane Mode of Flight," Proceedings of the 57th Annual AHS Forum, Washington, DC, May 9–11, 2001.
10. Nixon, M. W., Langston, C. W., Singleton, J. D., Piatak, D. J., Kvaternik, R. G., Corso, L. M., and Brown, R., "Aeroelastic Stability Of A Soft-Inplane Gimballed Tiltrotor Model In Hover," Proceedings of the 42nd AIAA/ASME/ASCE/AHS/ASC Structures, Structural Dynamics, and Materials Conference, Seattle, Washington, April 16–19, 2001.
11. Nixon, M. W., Langston, C. W., Singleton, J. D., Piatak, D. J., Kvaternik, R. G., Corso, L. M., and Brown, R. K., "Technical Note: Hover Test of a Soft-Inplane Gimballed Tiltrotor Model," *Journal of the American Helicopter Societ*y, vol. 48, no. 1, January 2003, pp. 63–66.
12. Kvaternik, R. G., "Exploratory Studies in Generalized Predictive Control for Active Aeroelastic Control of Tiltrotor Aircraft," NASA TM-2000-210552.
13. Hathaway, E., and Gandhi, F., "Tiltrotor Whirl Flutter Alleviation Using Actively Controlled Wing Flaperons," Presented at the AHS International 60th Annual Forum and Technology Display, Baltimore, Maryland, June 7–10, 2004.
14. Singh, R., Hathaway, E.L. and Gandhi, F., "Comparison of Wing-Flaperon and Swashplate Actuation for Tiltrotor Whirl Flutter Stability Augmentation", to be presented at the 46th AIAA/ASME/ASCE/AHS/ASC Structures, Structural Dynamics & Materials Conference, Austin, Texas, 18 - 21 April 2005.
15. Nixon, M. W., Kvaternik, R. G., and Settle, T. B., "Tiltrotor Vibration Reduction Through Higher Harmonic Control," Proceedings of the 53rd Annual AHS Forum, Virginia Beach, Virginia, April 29– May 1, 1997.
16. Hathaway, E. L. and Gandhi, F., "Modeling Refinements in Simple Tiltrotor Whirl Flutter Analyses," *Journal of the American Helicopter Societ*y, vol. 48, no. 3, July 2003, pp. 186–198.
17. Hathaway, E. L.., *Active and Passive Techniques for Tiltrotor Aeroelastic Stability Augmentation*, Ph.D. thesis, The Pennsylvania State University, 2005.
18. Hathaway, E. and Gandhi, F., "Design Optimization for Improved Tiltrotor Whirl Flutter Stability," Proceedings of the 29th European Rotorcraft Forum, Friedrichshafen, Germany, 16–18 September 2003.
19. Gandhi, F., and Hathaway, E., "Optimized Aeroelastic Couplings for Alleviation of Helicopter Ground Resonance," *Journal of Aircraft*, Vol. 35, No. 4, July-August 1998, pp. 582-590.
20. Hathaway, E., and Gandhi, F., "Concurrent Optimization of Aeroelastic Couplings and Rotor Stiffness for the Alleviation of Helicopter Aeromechanical Instability," *Journal of Aircraft*, Vol. 38, No. 1, Jan.-Feb. 2001, pp. 69-80.

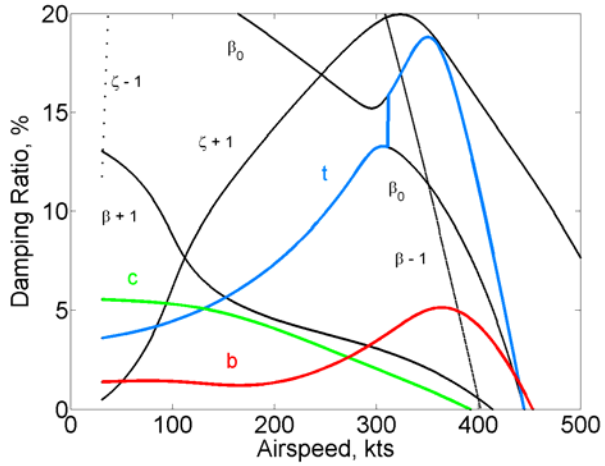

Figure 1: Modal damping vs. airspeed at cruise (386) RPM – baseline, no-control case

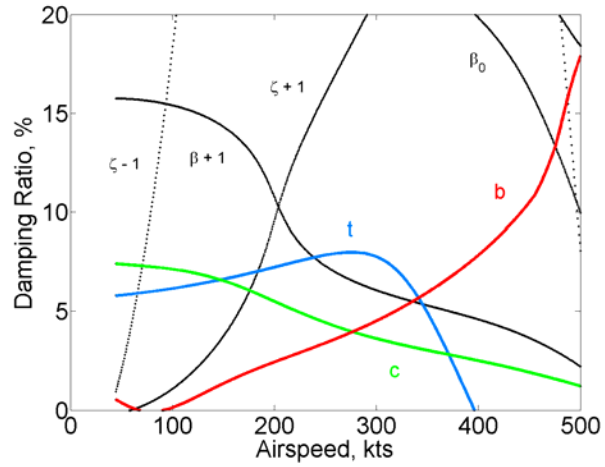

Figure 2: Modal damping vs. airspeed at hover (551) RPM – baseline, no-control case

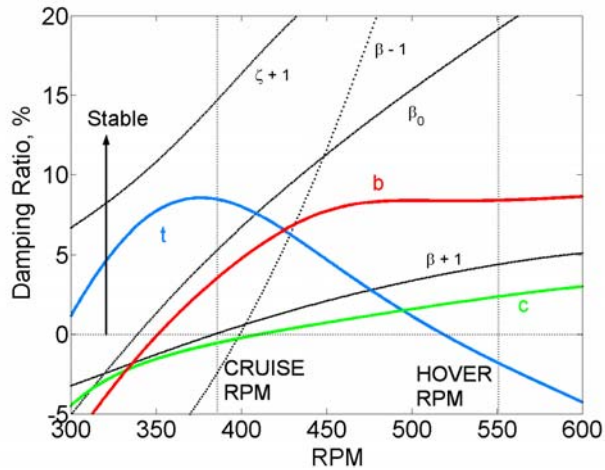

Figure 3: Modal damping vs. RPM at 410 kts – baseline, no-control case

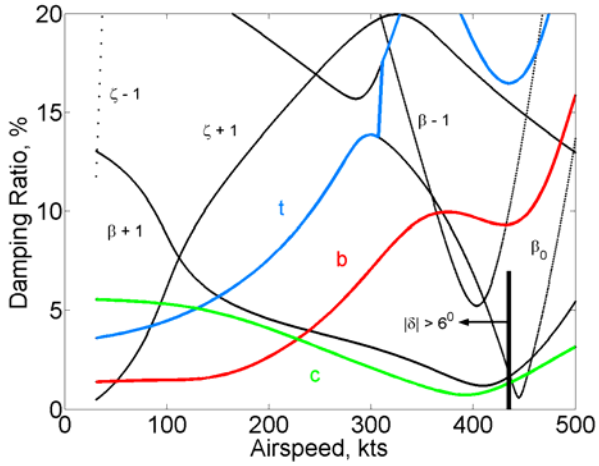

Figure 4: Modal damping vs. airspeed at cruise (386) RPM with LQR optimal wing flaperon control

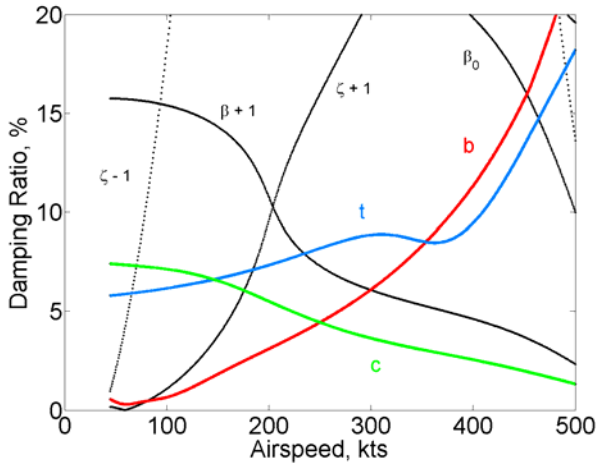

Figure 5: Modal damping vs. airspeed at hover (551) RPM with LQR optimal wing flaperon control

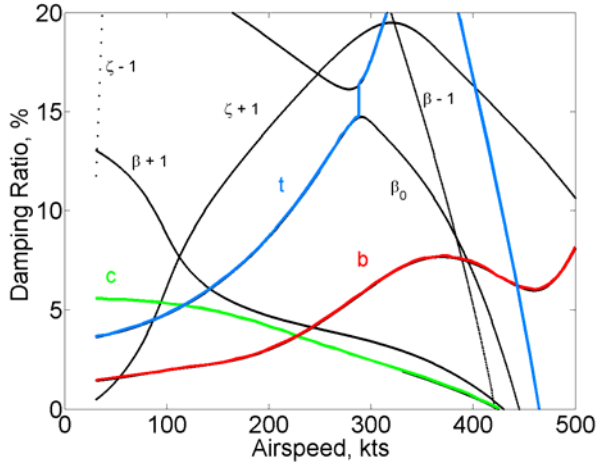

Figure 6: Modal damping vs. airspeed at cruise (386) RPM, flaperon input based on scaled constant gains (optimal at 386 RPM, 410 kts) from Fig. 4

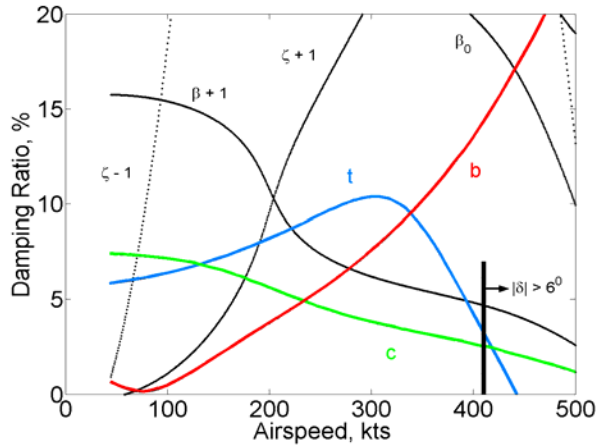

Figure 7: Modal damping vs. airspeed at hover (551) RPM, flaperon input based on scaled constant gains (optimal at 386 RPM, 410 kts) from Fig. 4

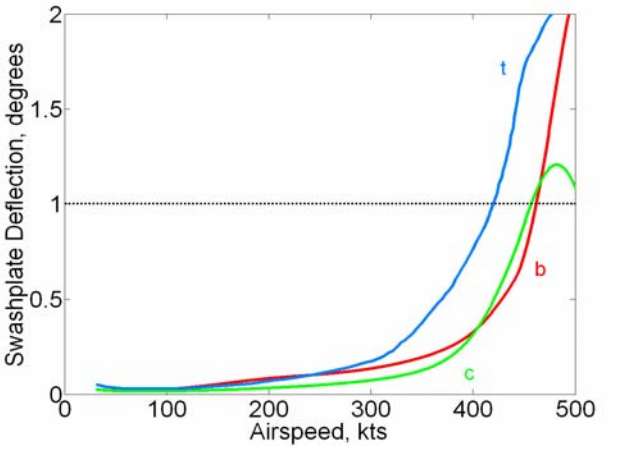

Figure 10: Swashplate deflection vs. airspeed at cruise (386) RPM with LQR optimal swashplate control

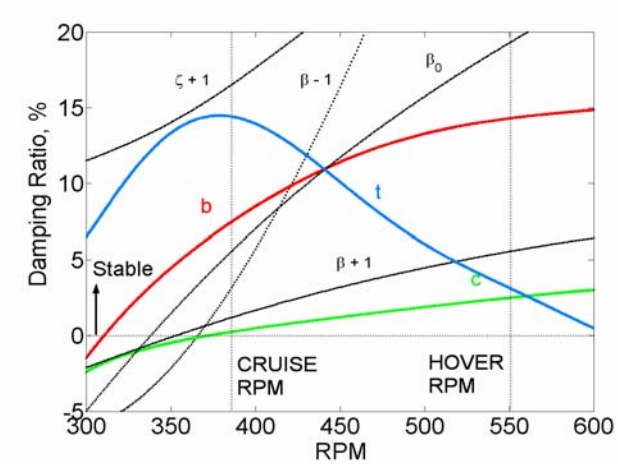

Figure 8: Modal damping vs. RPM at 410 kts, flaperon input based on scaled constant gains (optimal at 386 RPM, 410 knots) from Fig. 4

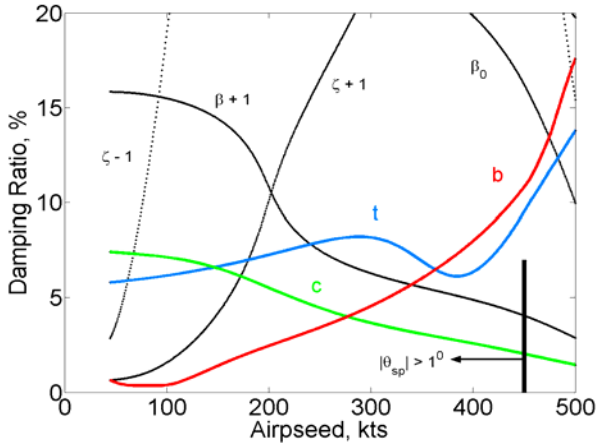

Figure 11: Modal damping vs. airspeed at hover (551) RPM with LQR optimal swashplate control

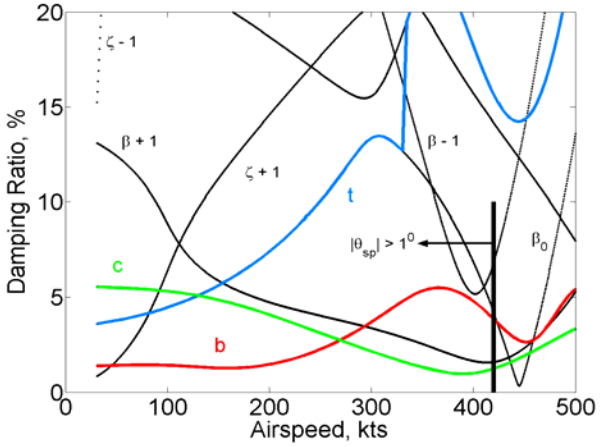

Figure 9: Modal damping vs. airspeed at cruise (386) RPM with LQR optimal swashplate control

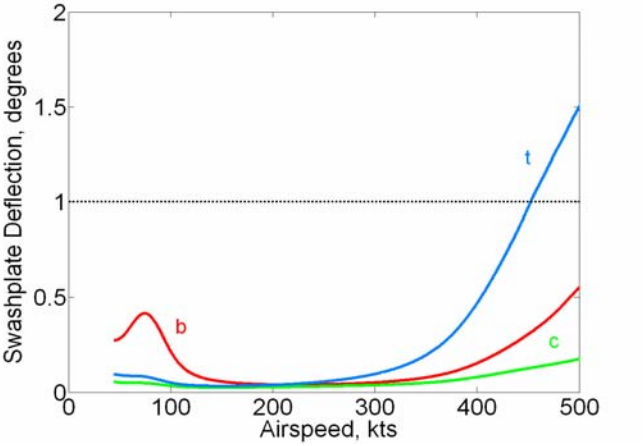

Figure 12: Swashplate deflection vs. airspeed at hover (551) RPM with LQR optimal swashplate control

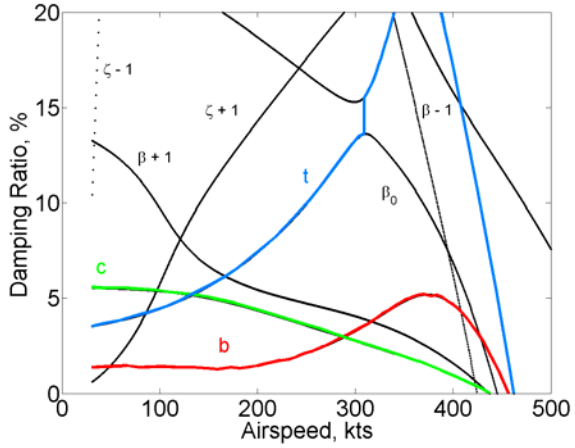

Figure 13: Modal damping vs. airspeed at cruise (386) RPM, swashplate input based on scaled constant gains (optimal at 386 RPM, 410 kts) from Fig. 9

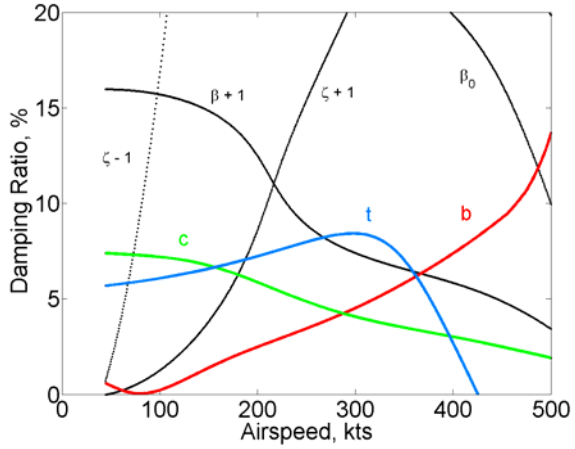

Figure 14: Modal damping vs. airspeed at hover (551) RPM, swashplate input based on scaled constant gains (optimal at 386 RPM, 410 kts) from Fig. 9

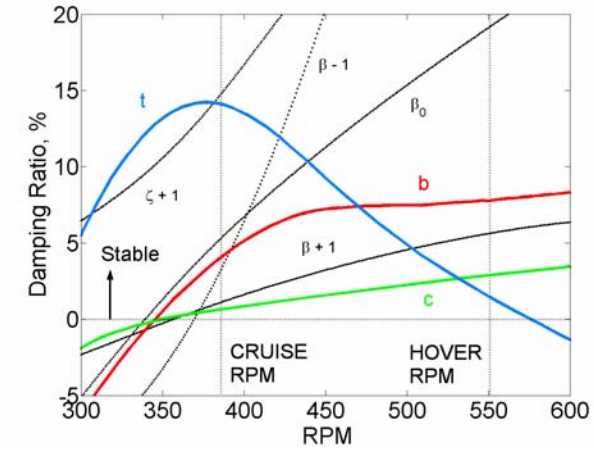

Figure 15: Modal damping vs. RPM at 410 kts, swashplate input based on scaled constant gains (optimal at 386 RPM, 410 knots) from Fig. 9

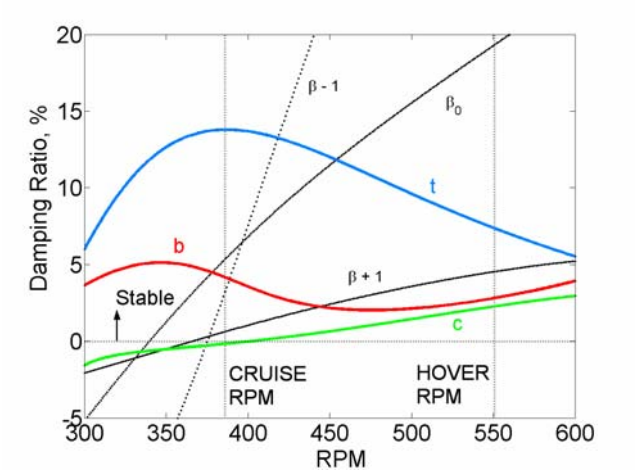

Figure 16: Modal damping vs. RPM at 410 kts; flaperon input based on wing-state feedback; gains from moving-point optimization; ±6 deg limits

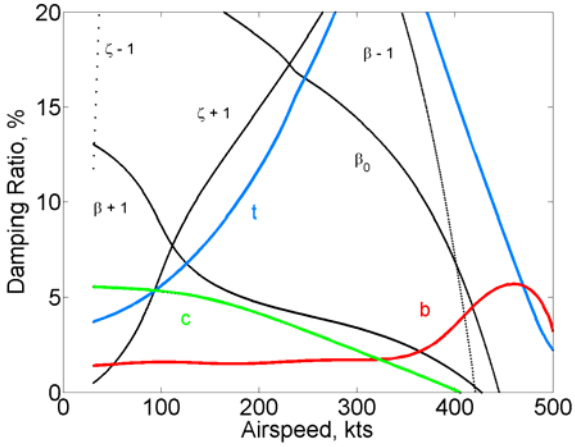

Figure 17: Modal damping vs. airspeed at cruise (386) RPM, flaperon input based on wing-state feedback; gains from Fig. 16

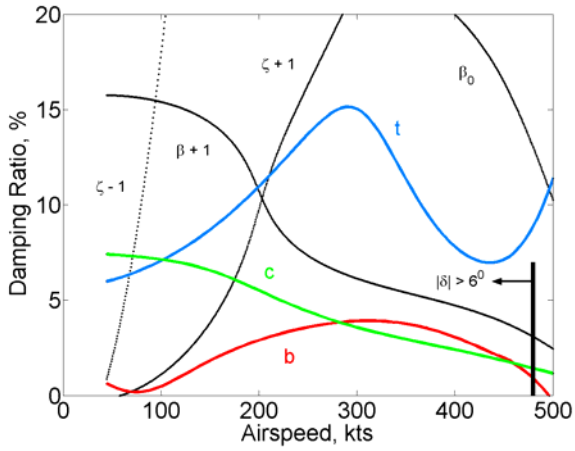

Figure 18: Modal damping vs. airspeed at hover (551) RPM, flaperon input based on wing-state feedback; gains from Fig. 16

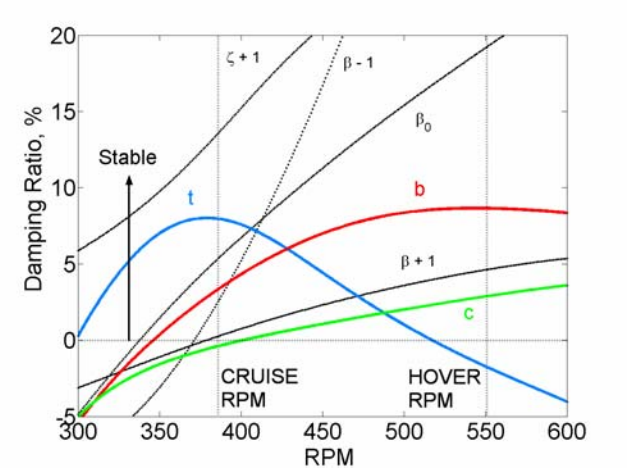

Figure 19: Modal damping vs. RPM at 410 kts; swashplate input based on wing-state feedback; gains from moving-point optimization; ±1 deg limit

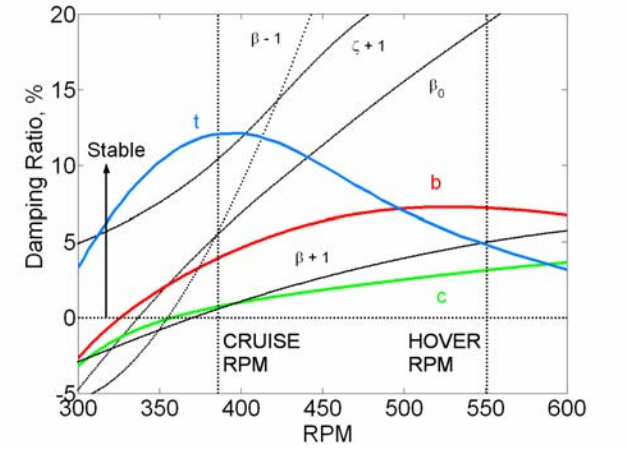

Figure 20: Modal damping vs. RPM at 410 kts; swashplate input based on wing-state feedback; gains from moving-point optimization; ±2 deg limit